ELSEVIER

Biochemical Pharmacology 65 (2003) 349–360

Biochemical Pharmacology

www.elsevier.com/locate/biochempharm

Lipophilicity of analogs of pyridoxal isonicotinoyl hydrazone (PIH) determines the efflux of iron complexes and toxicity in K562 cells

Joan L. Buss, Emmanuele Arduini, Kyle C. Shephard, Prem Ponka*

Departments of Physiology and Medicine, McGill University, and Lady Davis Institute for Medical Research, Sir Mortimer B. Davis Jewish General Hospital, 3755 Chemin de la Cote-Ste-Catherine, Montreal, Que., Canada H3T 1E2

Received 27 March 2002; accepted 5 July 2002

Abstract

Iron overload secondary to β-thalassemia and other iron-loading anemias is the most serious obstacle to be overcome in the treatment of these diseases, since there is no physiological mechanism for excretion of the excess iron acquired by chronic blood transfusion. Due to the inconvenience and cost of the current iron chelation therapy, the search for an orally available iron chelator is ongoing. Pyridoxal isonicotinoyl hydrazone (PIH) and many of its analogs are effective at mobilizing iron *in vivo* and *in vitro* at doses that are not toxic. PIH analogs were approximately equally effective at binding ^{59}Fe within K562 cells; their efficacy depended upon the kinetics of release of the iron–chelator complex from the cell, which was correlated inversely with the lipophilicity of the chelators. Addition of BSA, which has a well-characterized affinity for lipophilic species, to the extracellular medium enhanced iron–chelator efflux, such that all analogs caused ^{59}Fe release from the cells as quickly as it was chelated; this suggests that BSA acts as an extracellular sink for the iron–chelator complexes, many of which are highly lipophilic. The toxicity of the free chelators varied over two orders of magnitude, and was correlated with the amount of intracellular ^{59}Fe–chelator complexes, implicating the complexes in the mechanism of toxicity of the chelators. Understanding the structural features that determine the efficacy and toxicity of iron chelators in biological systems is of value in the selection of PIH analogs for *in vivo* examination.

Keywords: Toxicity of iron chelators; Lipophilicity; Pyridoxal isonicotinoyl hydrazone (PIH); PIH analogs; Iron chelators; Mobilization of iron from cells

1. Introduction

The importance of iron in biological systems is due mainly to its roles in oxygen distribution and electron transfer. Iron in excess of the capacity of the organism to use or store it is toxic, presumably via formation of reactive oxygen species, including the extremely reactive hydroxyl radical [1], which cause oxidative stress. To prevent uncontrolled redox reactions, and to conserve a poorly bioavailable metal, iron metabolism in mammals is tightly regulated, and involves efficient recycling [2]. Because there is no physiological mechanism of iron excretion, patients receiving chronic blood transfusions develop iron overload, the current treatment for which is desferrioxamine, a drug that must be administered via subcutaneous infusion [3] due to its very short plasma half-time [4].

An orally effective iron chelator is urgently needed as a convenient and inexpensive alternative to desferrioxamine therapy. The efficacy of PIH (Fig. 1) in iron mobilization has been characterized *in vitro* [5] and *in vivo* [6]. Screens of PIH analogs using ^{59}Fe-labeled cell culture models have identified several chelators in this series that are more active than PIH [7–9], including pyridoxal *para*-methoxybenzoyl hydrazone, pyridoxal *meta*-chlorobenzoyl hydrazone (*m*-ClPBH), and pyridoxal *meta*-fluorobenzoyl hydrazone (*m*-FPBH). These analogs also mobilized more ^{59}Fe in rats than PIH, whether administered intraperitoneally or orally

* Corresponding author. Tel.: +1-514-340-8222, Ext. 5289; fax: +1-514-340-7502.

E-mail address: prem.ponka@mcgill.ca (P. Ponka).

Abbreviations: ClPBH, pyridoxal chlorobenzoyl hydrazone; FBS, fetal bovine serum; FPBH, pyridoxal fluorobenzoyl hydrazone; LIP, labile iron pool; MEM, minimal essential medium; MTS 3-(4,5-dimethylthiazol-2-yl)-5-(3-carboxymethoxyphenyl)-2-(4-sulfophenyl)-2*H*-tetrazolium; PBH, pyridoxal benzoyl hydrazone; PIH, pyridoxal isonicotinoyl hydrazone; PMS, phenomethazine sulfonate.

0006-2952/02/$ – see front matter © 2002 Elsevier Science Inc. All rights reserved.
PII: S0006-2952(02)01551-4

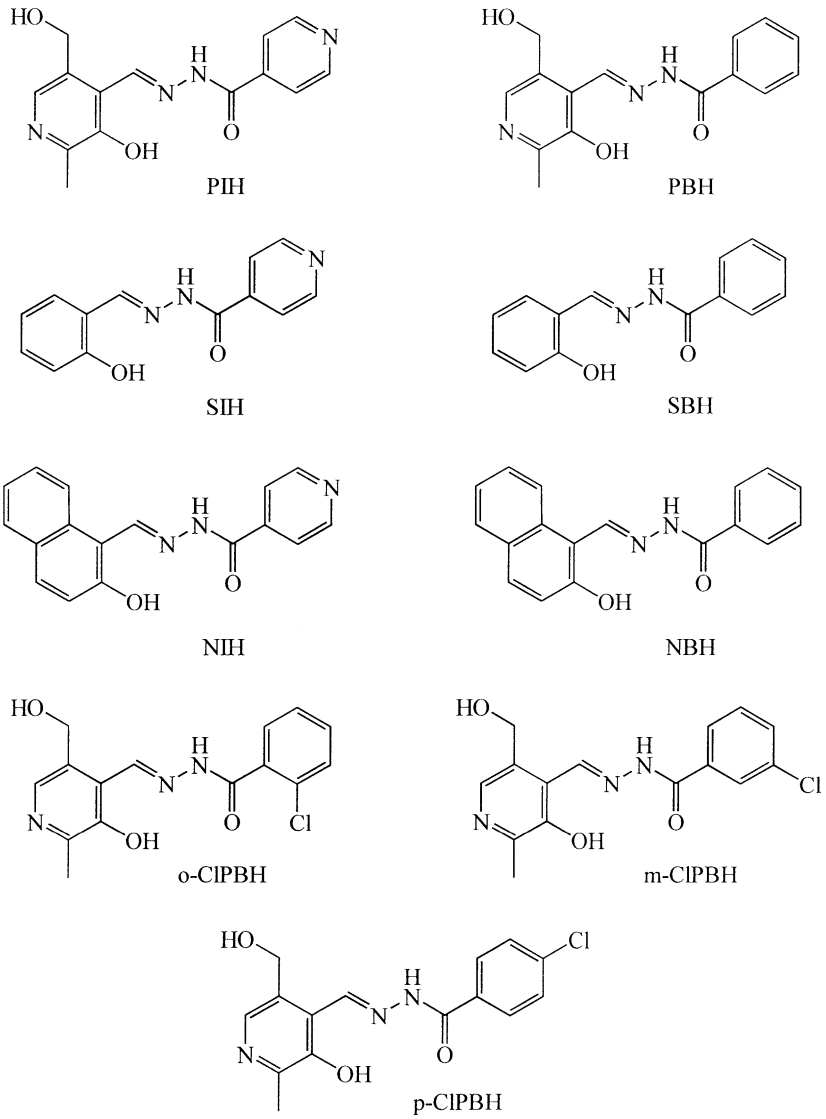

Fig. 1. Structures of the chelators examined: pyridoxal isonicotinoyl hydrazone (PIH), pyridoxal benzoyl hydrazone (PBH), salicylaldehyde isonicotinoyl hydrazone (SIH), salicylaldehyde benzoyl hydrazone (SBH), 2-hydroxy-1-naphthylaldehyde isonicotinoyl hydrazone (NIH), 2-hydroxy-1-naphthylaldehyde benzoyl hydrazone (NBH) and the positional isomers of pyridoxal chlorobenzoyl hydrazone (ClPBH).

[10]. A recent study has demonstrated that the property defining the capacity of PIH analogs to mobilize ^{59}Fe from reticulocytes is the rate of efflux of the iron–chelator complexes from the cells [11], presumably via passive diffusion. It is of interest whether these chelators mobilize ^{59}Fe similarly from other cell lines, which, as compared with reticulocytes, may be expected to have different intracellular pathways of iron trafficking.

Several studies have demonstrated the antiproliferative effects of some PIH analogs in cell culture models [8,12–15]. It has been demonstrated that ^{59}Fe mobilization and inhibition of DNA synthesis were not correlated [16], suggesting that iron depletion from cells, which is expected to limit the iron available to ribonucleotide reductase, is insufficient to account for the antiproliferative effects of these chelators. Hence, it is of value to examine other mechanisms by which the toxicity of PIH analogs may be mediated.

2. Materials and methods

2.1. Synthesis of PIH analogs

Pyridoxal hydrochloride was purchased from Sigma. Salicylaldehyde and 2-hydroxy-1-naphthylaldehyde were purchased from Aldrich. Isonicotinic acid hydrazide and benzoyl hydrazide were purchased from Lancaster. The halogenated acid benzoyl hydrazides used for preparation of the hydrazones were purchased from Transworld Chemicals. PIH and its analogs were synthesized according to standard methods as previously described [17]. All other materials were of the highest quality available.

2.2. Preparation of chelator and Fe(chelator)$_2$ solutions

Stock solutions of the chelators were prepared in either NaOH or HCl, and either were used immediately or stored

at −20°. These frozen solutions did not hydrolyze significantly over at least 6 months of storage, as assessed spectrophotometrically. Stock solutions of Fe(chelator)$_2$ complexes were prepared at a minimum concentration of 25 μM by the addition of 5 mM $FeCl_3$ (Fisher) in 100 mM sodium citrate (Bioshop) and chelator in a 1:2 molar ratio, and incubated at room temperature for 60 min. That these incubation conditions were sufficient to allow complete complex formation was confirmed spectrophotometrically.

2.3. ^{59}Fe mobilization from K562 cells

K562 cells were cultured in RPMI (Gibco) supplemented with 10% FBS (Gibco). Cells from log phase cultures were labeled with ^{59}Fe by incubating 10^7 cells/mL with 10 μM $^{59}Fe_2$–transferrin, prepared as previously described from human apotransferrin (Sigma) and $^{59}FeCl_3$ (Amersham), in RPMI supplemented with 1% FBS for 3 hr [18]. Washed ^{59}Fe-labeled cells (the radioactivity of which corresponds to 100% in Figs. 3–7) were incubated in 6-well plates (Canadian Life Technologies) with chelators at a density of 10^6 cells/mL as described for each experiment, and were centrifuged at 210 *g* for 5 min at 4°. Ethanol-soluble cytosolic fractions, which contain ^{59}Fe bound to cellular ligands and chelators, were separated from ethanol-insoluble material, including proteins, by lysing the cells with 200 μL of cold double-distilled water and 1 mL of ice-cold 95% ethanol, and centrifuging at 1800 *g* for 20 min at 4° [18]. Radioactivity was measured in samples of the extracellular medium and ethanol-soluble and -insoluble fractions, and the total of these three fractions was summed to confirm that radioactivity had not been lost during sample handling.

When ^{59}Fe-labeled cells were washed and incubated for 2 hr in MEM in the absence of chelators, approximately 10% of the ^{59}Fe was released into the medium, probably due to the release of a small amount of $^{59}Fe_2$–transferrin from which ^{59}Fe was not dissociated during the labeling period. To simplify the figures, data shown in the time- and concentration-dependent experiments were corrected for this non-specific ^{59}Fe release by subtraction of the ^{59}Fe released from identically treated control samples.

Generally, within each experiment, variability among identically prepared samples was extremely low. Variability among experiments was somewhat greater, probably due to non-uniform levels of non-heme ^{59}Fe in various reticulocyte preparations. To assess variability among experiments, PIH was used as a control in each experiment to assess reproducibility [18]. In five independent experiments, ^{59}Fe mobilization by 100 μM PIH during a 2-hr incubation was 22 ± 4% (average ± SD). Since the effect of PIH was similar in all experiments in this study, comparisons among the experiments can be made safely.

2.4. Toxicity of chelators and Fe(chelator)$_2$ complexes toward K562 cells

Acute effects of the chelators were assessed in triplicate by trypan blue exclusion after a 2-hr incubation period in PBS, with and without 5% BSA (Sigma), in 6-well plates. Cell viability in the presence of chelators over 72 hr was measured using the MTS assay (Promega). MTS and PMS (purchased from Aldrich) in the presence of cells with active mitochondrial dehydrogenase cause the reduction of MTS to a water-soluble product, the concentration of which can be measured spectrophotometrically to indirectly measure cell number. MTS assays were performed in 200-μL volumes in 96-well plates (Falcon) seeded with 14,000 cells/well, and absorbance measurements were made at 492 nm using a Titertek Multiscan plate reader (MTX Lab Systems). The MTS assay was calibrated against cell number to ensure a linear relationship between mitochondrial dehydrogenase activity over the range of cell densities used in the experiments. Since the results of the MTS assay did not accurately reflect cell number when K562 cells were treated with iron–chelator complexes, cell viability in the presence of Fe(chelator)$_2$ over 72 hr was assessed by trypan blue exclusion. These experiments were performed in 24-well plates (Nunc) in quadruplicate. Cells, taken from log phase cultures, were seeded at a density of 10^5/mL, and the final volume in the wells was 500 μL.

2.5. Partition coefficients of chelators

Ethyl acetate/PBS partition coefficients were determined spectrophotometrically. The wavelengths chosen for analysis (325–385 nm) were local maxima. Partition coefficients were calculated from the absorbances of the chelators dissolved in ethyl acetate-saturated PBS before and after the addition of measured quantities of ethyl acetate. Volumes of ethyl acetate were chosen such that no more than 90% and no less than 10% of the chelator entered the organic phase. Experiments were performed in triplicate.

3. Results

3.1. ^{59}Fe mobilization from K562 cells

K562 cells were labeled with ^{59}Fe by incubation for 3 hr with $^{59}Fe_2$–transferrin as described in Section 2. After this period of incubation, ^{59}Fe is distributed between ferritin, the major iron storage protein, and the poorly characterized LIP [15]. The steps involved in ^{59}Fe mobilization, defined in Fig. 2, were examined separately after the incubation of cells with the chelators by measuring the radioactivity in the incubation medium and in an ethanol-soluble cytoplasmic fraction, which presumably represents ^{59}Fe–chelator

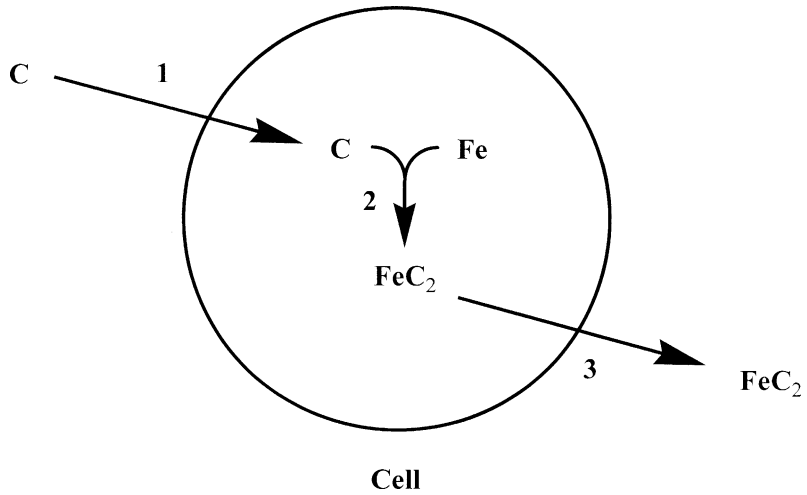

Fig. 2. Scheme of the steps involved in iron mobilization: diffusion of the chelator (C) into the cell (1), binding cellular iron (2), and release of the iron–chelator complex from the cell (3). The term ''mobilization'' refers to the sum of steps (1) to (3).

that remains in the cell [18]. Thus, it is possible to evaluate the capacities of the chelators to both bind ^{59}Fe and release the ^{59}Fe–chelator complexes from the cells.

The kinetics of ^{59}Fe mobilization from K562 cells by 100 μM PIH analogs (structures shown in Fig. 1) were examined (Figs. 3 and 4). The kinetics of ^{59}Fe binding were similar for all analogs; they bound 25–40% of the total ^{59}Fe in the cells after a 60-min incubation, while PIH bound approximately 20%. The kinetics of ^{59}Fe mobilization were quite fast; the half-times were less than 15 min, and the process was complete in 60 min. PIH, *o*-ClPBH, and *o*-ClSBH caused a low, transient accumulation of ^{59}Fe–chelator (Figs. 3 and 4) in the cytosol, which appeared to be due to the relatively fast efflux of ^{59}Fe from the cell such

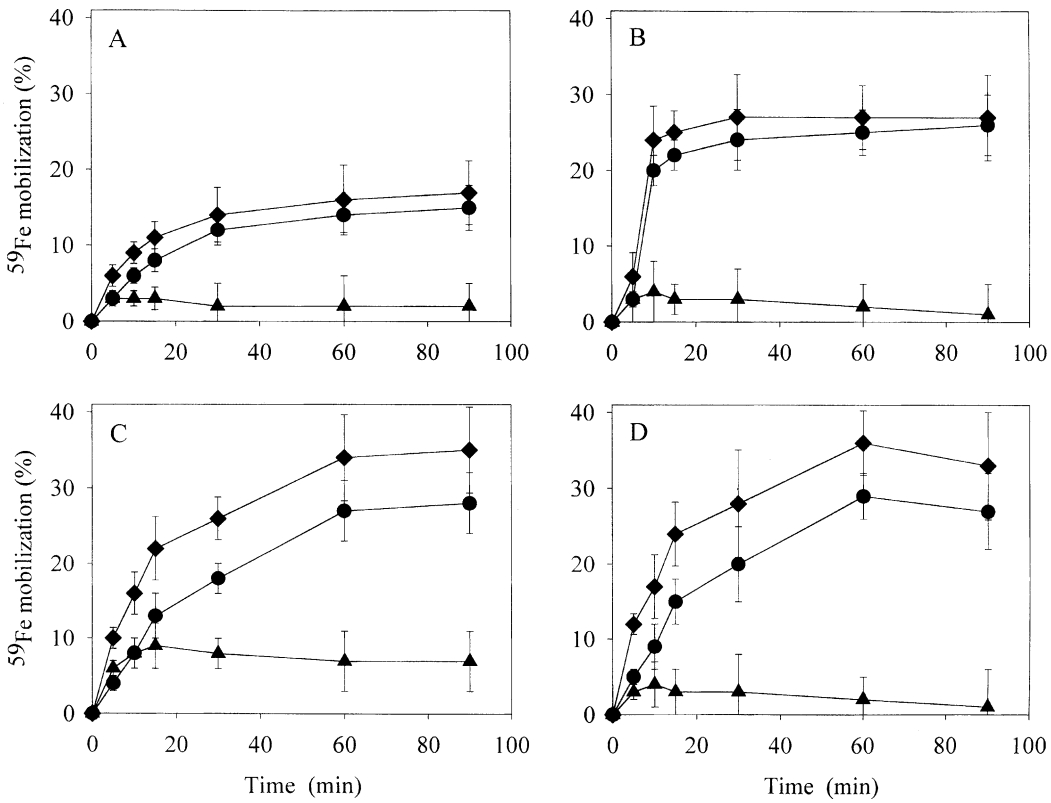

Fig. 3. Kinetics of ^{59}Fe binding and release from ^{59}Fe-labeled K562 cells by 100 μM PIH (A), *o*-ClPBH (B), *m*-ClPBH (C), and *p*-ClPBH (D). Data are corrected for ^{59}Fe release that is not chelator-mediated by the subtraction of control values for each incubation time. Error bars represent SD of triplicate measurements. Key: (◆) total ^{59}Fe bound (i.e. the sum of ethanol-soluble and released ^{59}Fe), (●) ^{59}Fe released into the incubation medium, and (▲) intracellular ethanol-soluble ^{59}Fe.

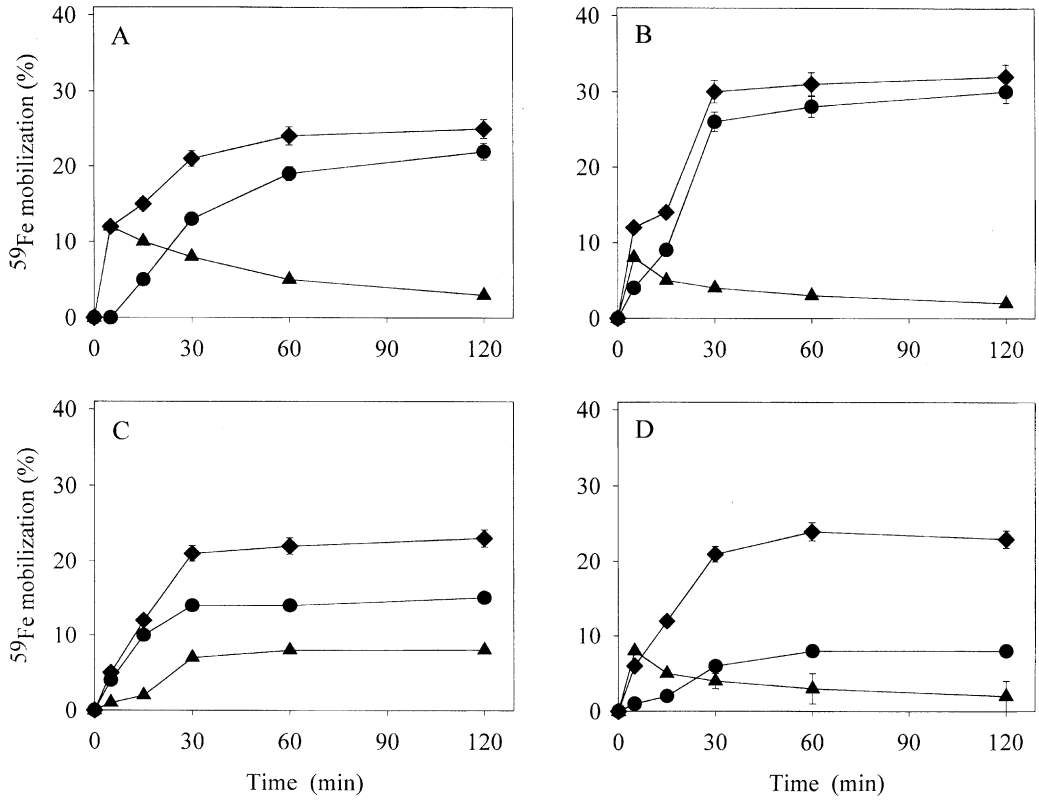

Fig. 4. Kinetics of ^{59}Fe binding and release from ^{59}Fe-labeled K562 cells by 100 μM PIH (A), *o*-ClSBH (B), *m*-ClSBH (C), and *p*-ClSBH (D). Error bars represent SD of triplicate measurements. Data are corrected for ^{59}Fe release that is not chelator-mediated by the subtraction of control values for each incubation time. Key: (◆) total ^{59}Fe bound (i.e. the sum of ethanol-soluble and released ^{59}Fe), (●) ^{59}Fe released into the incubation medium, and (▲) intracellular ethanol-soluble ^{59}Fe.

that, after 60 min, essentially all chelator-bound ^{59}Fe had been released from the cell. In contrast, the *meta* and *para* isomers released ^{59}Fe more slowly; after a 2-hr incubation, much higher levels of ^{59}Fe remained in the ethanol-soluble cytosolic fraction, presumably as iron–chelator complexes. The ClPBH and ClSBH analogs bound similar amounts of cellular ^{59}Fe, and the differences in their capacities to mobilize ^{59}Fe depended on the kinetics of efflux of their ^{59}Fe–chelator complexes.

The concentration dependence of ^{59}Fe binding by PIH was markedly different from the ClSBH analogs (Fig. 5). All three ClSBH isomers were approximately equally effective at binding ^{59}Fe, and their effects were maximal at 10 μM. At all chelator concentrations, approximately half of the ^{59}Fe bound by *m*- and *p*-ClSBH was released into the incubation medium during the 3-hr incubation, while nearly all ^{59}Fe bound by *o*-ClSBH and PIH was released. ^{59}Fe binding by PIH increased with concentration over the range assessed in this experiment, and much higher concentrations of PIH were required to achieve the levels of ^{59}Fe binding observed for the ClSBH isomers. This weaker concentration dependence of PIH in comparison to its analogs has also been demonstrated in reticulocytes [11], in which the effects of ClPBH and FPBH analogs are maximal at concentrations above 50 μM, while ^{59}Fe mobilization by PIH increases linearly over this range.

To determine whether other *ortho*-halogenated PIH analogs were as efficient as *o*-ClSBH at mobilizing ^{59}Fe, a series of halogenated analogs were screened. At concentrations of 100 μM, the analogs bound approximately 40–50%

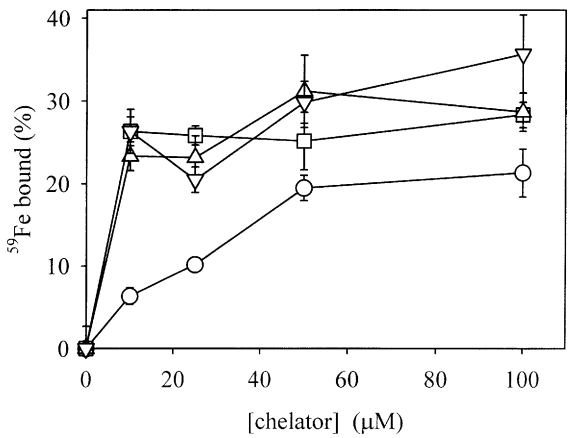

Fig. 5. Concentration dependence of ^{59}Fe binding from ^{59}Fe-labeled K562 cells by PIH analogs during a 3-hr incubation. Symbols represent total ^{59}Fe bound (i.e. the sum of ethanol-soluble and released ^{59}Fe) by PIH (○), *o*-ClSBH (□), *m*-ClSBH (△), and *p*-ClSBH (▽). For PIH and *o*-ClSBH, nearly all the radioactivity was found in the incubation medium, while approximately half that bound by *m*-ClSBH and *p*-ClSBH was found in the ethanol-soluble intracellular fraction. Data are corrected for ^{59}Fe release that is not chelator-mediated by the subtraction of control values. Error bars represent SD of triplicate measurements.

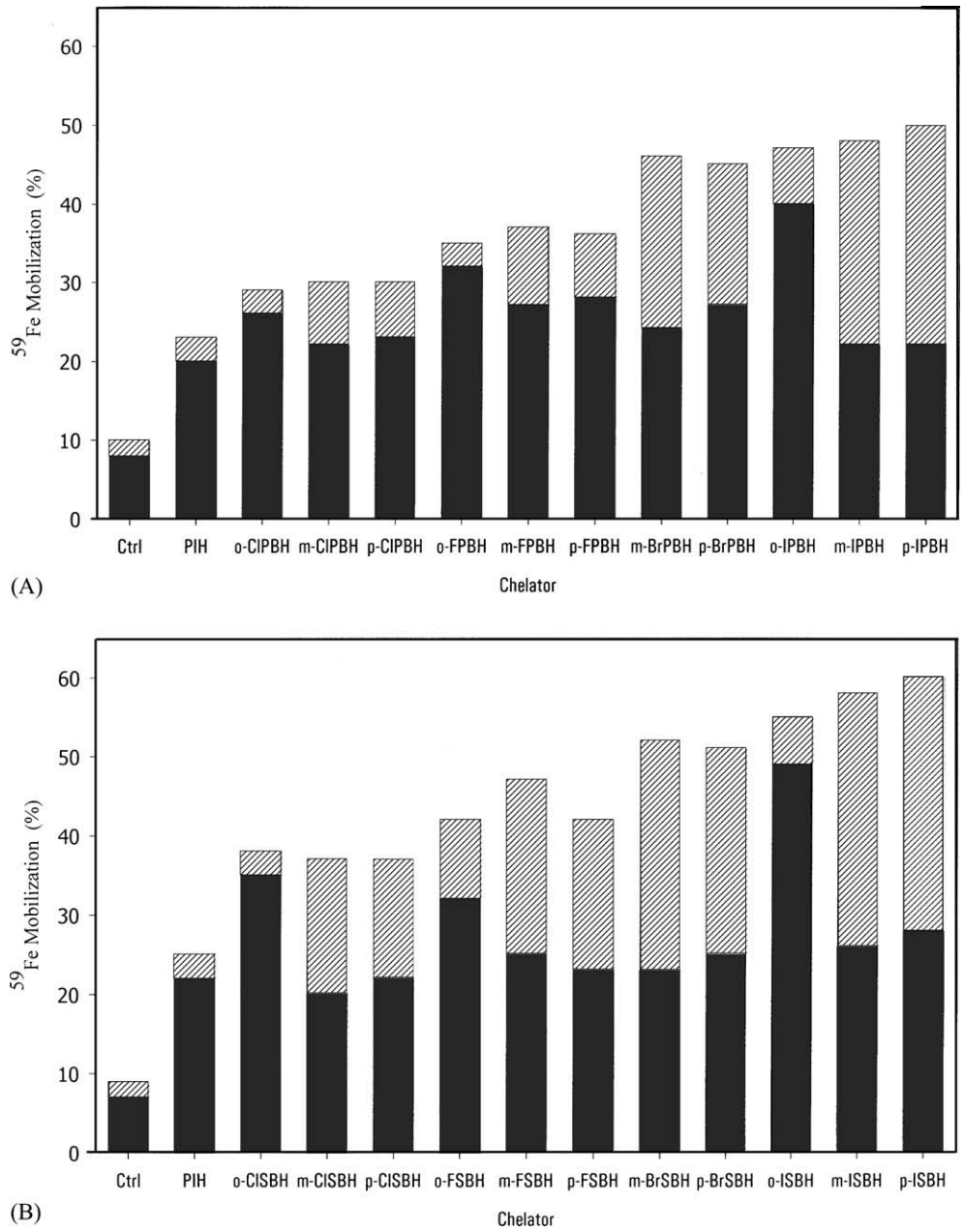

Fig. 6. ^{59}Fe binding and release from ^{59}Fe-labeled K562 cells by 100 μM chelators synthesized from pyridoxal (A) and salicylaldehyde (B). Incubations were for 2 hr at 37°. Key: black bars, ^{59}Fe released into the incubation medium; hatched bars, intracellular ethanol-soluble ^{59}Fe. Standard deviations in this experiment, which was performed twice, did not exceed 4%. IPBH = pyridoxal iodobenzoyl hydrazone; ISBH = salicylaldehyde iodobenzoyl hydrazone.

of the total cellular ^{59}Fe in 2 hr (Fig. 6), while PIH bound approximately 20%. The fraction of chelator-bound ^{59}Fe that was effluxed from the cell was much higher for the *ortho* isomers, and seems to be limited only by the kinetics of ^{59}Fe binding (Figs. 3 and 4).

It has been demonstrated that the iron complexes of the most lipophilic PIH analogs have high affinity for erythrocyte ghost membranes [11]; this has been proposed as the explanation for the slow efflux of lipophilic iron complexes [11]. The slow release of ^{59}Fe from reticulocytes by the *meta*- and *para*-substituted analogs, due to high membrane affinity, can be overcome by the addition of BSA to the incubation medium, which presumably acts as a sink by binding ^{59}Fe–chelator complexes as they are released from the cell [11]. Under these conditions, the PIH analogs examined release essentially all chelator-bound ^{59}Fe into the incubation medium [11]. Addition of 1% BSA to the incubation medium also had this effect on ^{59}Fe release from K562 cells by the chelators (Fig. 7). The total amount of ^{59}Fe bound by the chelators was not affected by the presence of BSA (Figs. 6 and 7), suggesting that, under these conditions, the binding of the chelators to BSA [11] did not inhibit the passive diffusion of chelator into the cell.

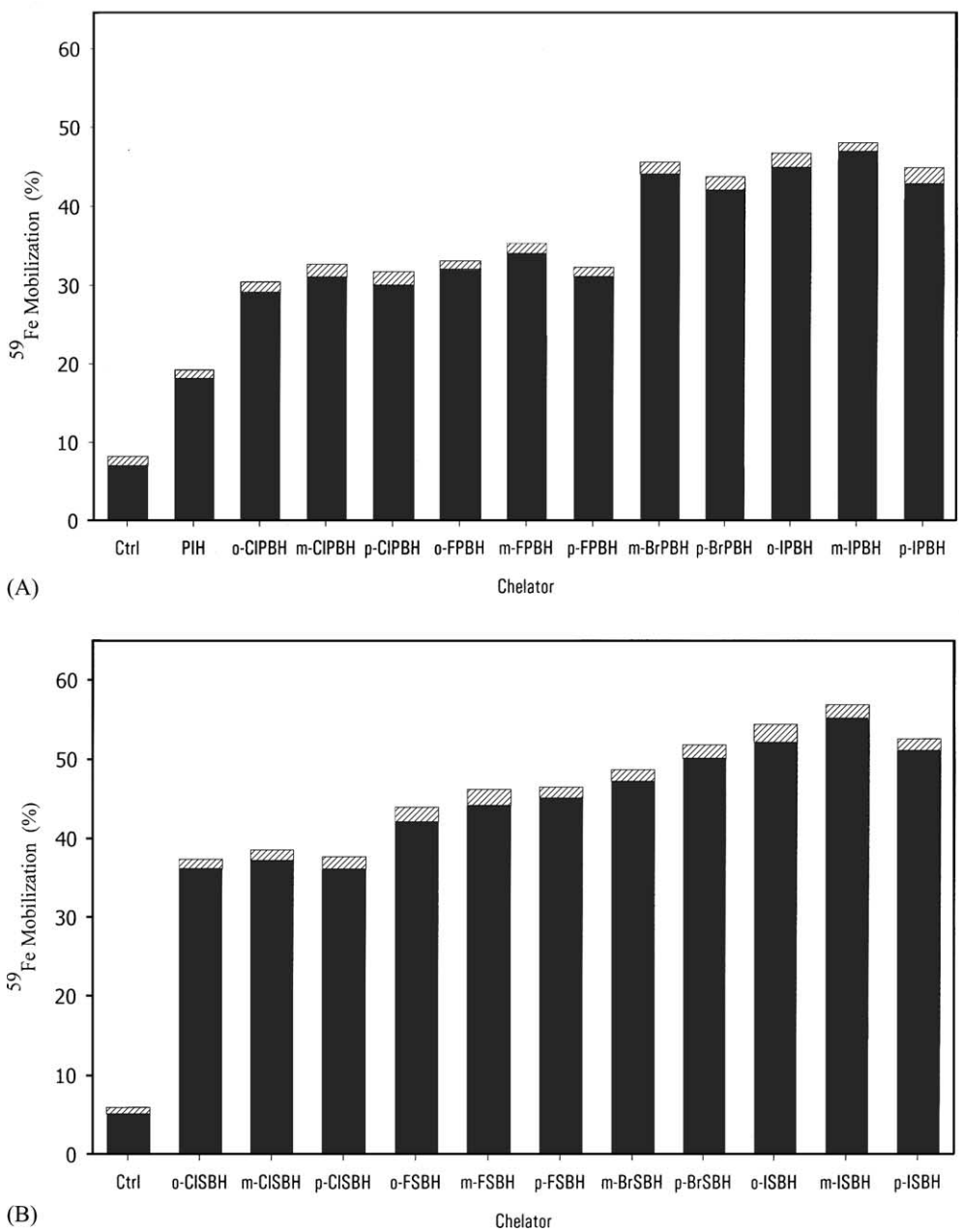

Fig. 7. ^{59}Fe binding and release from ^{59}Fe-labeled K562 cells by 100 μM chelators synthesized from pyridoxal (A) and salicylaldehyde (B) in the presence of 1% BSA. Incubations were for 2 hr at 37°. Key: black bars, ^{59}Fe released into the incubation medium; hatched bars, intracellular ethanol-soluble ^{59}Fe. Standard deviations in this experiment, which was performed twice, did not exceed 4%.

3.2. Toxicity of $Fe^{3+}(chelator)_2$ complexes toward K562 cells

The antiproliferative effects of the complexes were also examined. The ligands were incubated with Fe^{3+}-citrate as described in Section 2 to ensure complete complex formation before incubation of K562 cells with the complexes for 72 hr. Cell proliferation was assessed by trypan blue exclusion, and IC_{50} values were calculated by fitting the normalized data to a two-parameter logistic equation:

$$\text{Relative cell number} = \frac{1}{(c/IC_{50})^b + 1} \quad (1)$$

in which c is the chelator concentration, and b is the equivalent of the Hill coefficient. The IC_{50} values are reported in Table 1. While the IC_{50} values for the chelators varied over two orders of magnitude, those of the majority of their iron complexes fell into a much narrower range, with the exception of $FeSBH_2$, the most toxic of the complexes.

3.3. Toxicity of chelators toward K562 cells

The effect of exposure of K562 cells to 100 μM of the free chelators for 2 hr in PBS on cell viability was assessed by trypan blue exclusion (Table 1). The toxicity of the

Table 1
Toxicity of PIH analogs toward K562 cells[a]

	% Dead cells chelator 2 hr (trypan blue)	IC_{50} (μM) chelator 72 hr (MTS)	IC_{50} (μM) $Fe(chelator)_2$ 72 hr (trypan blue)
PIH	0	84 ± 4	24 ± 2
PBH	–[b]	39 ± 1	62 ± 2
o-ClPBH	1	51 ± 1	31.1 ± 0.3
m-ClPBH	6	15 ± 0.4	36 ± 1
p-ClPBH	7	13.2 ± 0.3	–
o-FPBH	1	55 ± 2	22 ± 2
m-FPBH	6	19.6 ± 0.5	24 ± 2
p-FPBH	5	21.0 ± 0.8	29 ± 2
m-BrPBH	9	–	–
p-BrPBH	10	–	–
o-IPBH	3	–	–
m-IPBH	11	–	–
p-IPBH	8	–	–
SIH	–	12.6 ± 0.6	17 ± 2
SBH	–	2.1 ± 0.1	0.96 ± 0.03
m-ClSBH	–	1.92 ± 0.06	–
m-FSBH	–	1.88 ± 0.09	–
NIH	–	1.12 ± 0.06	14 ± 2
NBH	–	1.00 ± 0.02	21 ± 1

[a] Values are means ± SD (N ranges from 3 to 7).
[b] Not determined.

chelators was relatively low, as was observed previously for 2-hydroxy-1-naphthylaldehyde isonicotinoyl hydrazone (NIH) at short incubation times with neuroblastoma cells [15], and the *meta*- and *para*-substituted PBH isomers were more toxic than the *ortho* isomers. The most toxic analog, *m*-IPBH, resulted in a loss of viability in 11% of the cells. In the presence of 1% BSA, no toxicity was observed for any of the chelators (data not shown). Though it is possible that membrane damage due to toxicity of the chelators may account for a small fraction of the ^{59}Fe release observed in the ^{59}Fe mobilization experiments (Figs. 3–7), this cannot be the only mechanism of ^{59}Fe release, since only a small percentage of cells had lost membrane integrity during a 2-hr incubation with the chelators. Moreover, it must be noted that the most toxic analogs, namely the *meta* and *para* isomers, caused the least release of ^{59}Fe, which is inconsistent with cell lysis as a major mechanism of ^{59}Fe release.

The toxicity of selected analogs was also assessed after a 72-hr incubation, and normalized data were fitted to Eq. (1). PIH had the weakest antiproliferative effect, with an IC_{50} of 84 μM, while the most toxic of the chelators examined had IC_{50} values two orders of magnitude lower. As was observed during the 2-hr incubation, the *meta*- and *para*-substituted analogs had significantly higher antiproliferative activity than their *ortho* isomers, which correlates with the affinity of their Fe^{3+} complexes for erythrocyte ghost membranes [11].

The antiproliferative effects of the ClPBH isomers were attenuated in the presence of 5% BSA, the level of albumin in human plasma, such that the IC_{50} values were approximately 2-fold higher (Fig. 8). Protection by BSA against

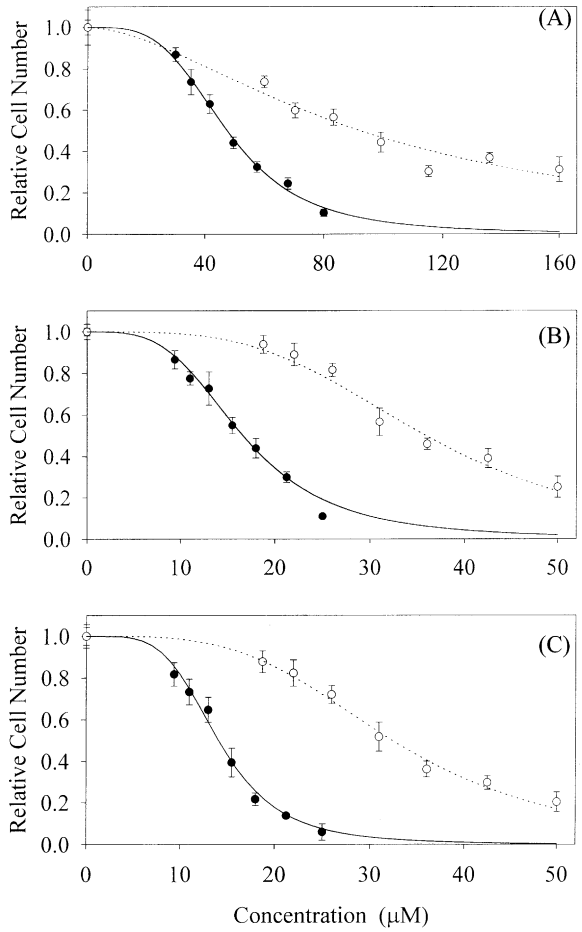

Fig. 8. Effect of BSA on the toxicity of ClPBH analogs. K562 cells were incubated with *o*-ClPBH (A), *m*-ClPBH (B), and *p*-ClPBH (C) for 72 hr in the absence (●) or presence (○) of 5% BSA. Cell viability was assessed by the MTS assay as described in Section 2. Error bars represent SD (N = 6). Experimental data were fitted to Eq. (1) (solid and dotted lines).

chelator toxicity was also observed at lower concentrations of BSA, although the effect was less pronounced (data not shown). Moreover, BSA completely prevented the toxicity observed after a 2-hr incubation of K562 cells with chelators. In the preceding experiments, it was demonstrated that BSA decreased the intracellular accumulation of ^{59}Fe–chelator complexes (Fig. 7). The inverse relationship between IC_{50} (Table 1) and the amount of ^{59}Fe found in the ethanol-soluble fraction after a 2-hr incubation with the chelators (Fig. 6) is shown in Fig. 9A. This relationship suggests a direct role of the complexes in mediating the toxicity of the chelators.

Ethyl acetate/PBS partition coefficients for some PIH analogs examined have been reported [19]. Experiments to determine those for PIH, PBH, SIH, and the *ortho* and *para* isomers of ClPBH and FPBH were performed as described in Section 2. Partition coefficients were calculated from absorbance data as follows:

$$P = \frac{y(1 - (A_x/A_0))}{x(A_x/A_0)} \quad (2)$$

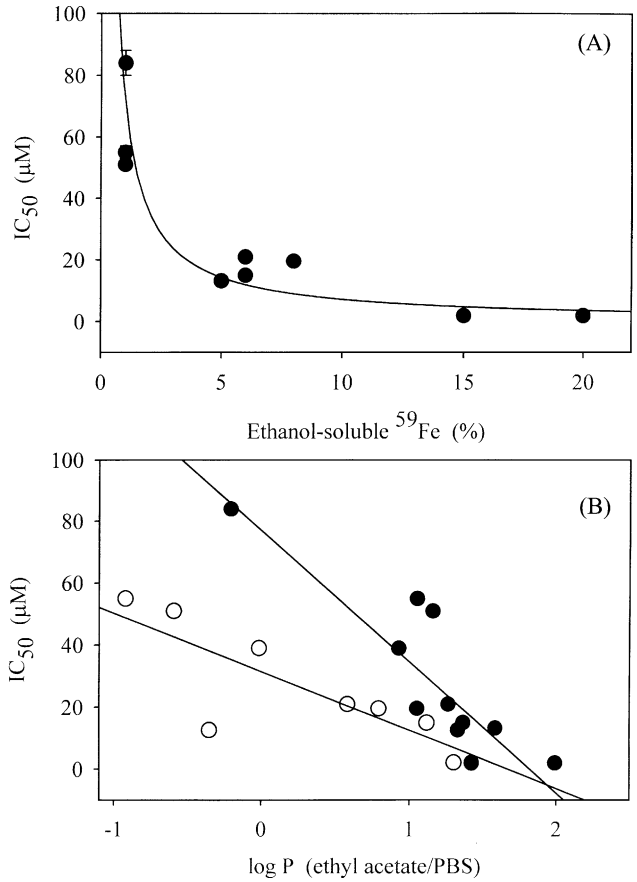

Fig. 9. Chelator toxicity, ^{59}Fe mobilization, and lipophilicity. (A) Toxicity (IC_{50} values from Table 1) is inversely correlated with intracellular ^{59}Fe (values from Fig. 6). The solid line is the least squares fit of the data to an equation of the form $y = ax^{-1}$. (B) Correlation of toxicity with lipophilicity of free chelators (●) and Fe^{3+} complexes (○). Solid lines represent linear, least squares fits of IC_{50} values and partition coefficients.

in which A represents the absorbance of the chelator in the PBS phase of volume y after the addition of a volume x of ethyl acetate. The partition coefficients of the free chelators determined in the present study were combined with those previously determined [19], since differences between values obtained by the two methods were not statistically significant. The complexes of *m*-FSBH, *m*-ClSBH, and *p*-ClPBH were insufficiently soluble to allow determination of their partition coefficients, and the very low lipophilicity of $FePIH_2$ also prevented a reliable determination.

The IC_{50} values were negatively correlated with the partition coefficients of both the free chelators and their Fe^{3+} complexes (Fig. 9B), and the slopes of the unweighted, linear, least-squares fits of these data were -42 ± 8 and -19 ± 5, respectively. That these slopes differ by a factor of approximately two is consistent with the predicted relationship between the lipophilicity of a free ligand and its 1:2 metal complex, a relationship that has been confirmed experimentally for many PIH analogs. The most likely explanation for the relationship between lipophilicity of the complexes and toxicity of the free ligands is a contribution of the iron–chelator complexes to the toxicity of the free chelators.

4. Discussion

4.1. ^{59}Fe mobilization in K562 cells by chelators

PIH analogs were effective in mobilizing ^{59}Fe from K562 cells, many of which were more effective than PIH itself (Fig. 6). At the concentrations used in this study, all chelators bound ^{59}Fe with similar kinetics (Figs. 3 and 4), but the kinetics of ^{59}Fe release from the cells varied markedly. The maximum amount of ^{59}Fe mobilized from K562 cells by 100 μM PIH analogs depended primarily upon the kinetics of release of ^{59}Fe–chelator complexes from the cells (Figs. 3, 4, and 6), which is determined by the lipophilicity of the complexes (Fig. 9A). It appears, therefore, that access of the chelators to intracellular compartments and binding of ^{59}Fe (steps 1 and 2 in Fig. 2) are equally efficient for all analogs, except PIH itself, which consistently bound the least ^{59}Fe. Since it has been demonstrated that PIH readily accesses intracellular compartments [18], the most likely explanation for the relatively low activity of PIH lies in its capacity to form iron complexes.

At low concentrations, the weaker activity of PIH was most apparent (Fig. 5). As the chelator concentration increased, ^{59}Fe mobilization by PIH increased, and approached that of the ClSBH analogs. Likely, PIH accesses the same intracellular iron pools as its analogs, only less effectively. Because of the relatively short incubation of cells with $^{59}Fe_2$–transferrin, a large fraction of the ^{59}Fe in K562 cells is expected to be in a transient pool, destined for incorporation into ferritin [20]. The fast kinetics of ^{59}Fe binding by PIH analogs (Figs. 3 and 4) are consistent with relatively weakly bound cellular ligands, the nature of which is unknown. It does not appear likely that PIH analogs are mobilizing ^{59}Fe from ferritin, since this process is slow *in vitro* [21], and because longer incubations with $^{59}Fe_2$–transferrin, which allow sufficient time for the majority of ^{59}Fe to reach ferritin, decrease ^{59}Fe mobilization by PIH analogs [15].

Structure–activity relationships describing the capacity of PIH analogs to mobilize ^{59}Fe from reticulocytes have been reported [11]. The reticulocyte model requires inhibition of heme synthesis, which prevents iron incorporation into heme, thereby enriching the non-heme iron pools. The capacities of these chelators to mobilize ^{59}Fe in this model, in which iron is targeted to the mitochondria, are similar to their effects on ^{59}Fe in K562 cells, which is mainly targeted to ferritin [15]. It is interesting that the structure–activity relationships describing the capacity of PIH analogs to mobilize ^{59}Fe hold for both cell types, despite the expected large differences in iron handling between them.

Since the chelators, with the exception of PIH, were equally effective at 10 and 100 μM at binding ^{59}Fe (Fig. 5),

pharmacologically achievable concentrations will likely be effective. ^{59}Fe mobilization occurred within 2 hr for the most effective analogs, which is consistent both with the results of similar experiments performed using reticulocytes [11], and with *in vivo* ^{59}Fe mobilization studies, which demonstrated that PIH mobilized ^{59}Fe from rats with a half-time of approximately 2 hr [6].

4.2. Toxicity of chelators and Fe(chelator)$_2$ complexes

The similar IC_{50} values obtained for most of the Fe(chelator)$_2$ complexes demonstrate that these species, with the exception of $FeSBH_2$ and $FeNBH_2$ (Table 1), are approximately equally able to prevent cell growth. Iron–PIH [22] and iron–SIH [23] complexes are known to donate iron to cells, and, at low concentrations, can be used to promote cell growth in iron-deficient medium. At higher concentrations, these complexes may donate iron in excess of the capacity of the cell to efficiently store or use it, resulting in iron accumulation in non-physiological pools [24]. Recently, $FeSIH_2$ and $FeNIH_2$ have been shown to induce apoptosis in Jurkat T lymphocytes, whereas $FePIH_2$ had no effect below its solubility limit [25]. Iron that is inappropriately handled by the cell may induce oxidative stress [1], even though the capacity of iron–PIH complexes to catalyze redox reactions appears to be much lower than that of iron–EDTA [26,27]. Another possible mechanism of growth inhibition is the inhibition of ribonucleotide reductase, which may be caused by the chelators themselves as demonstrated for NIH [28], or by their iron complexes as has been demonstrated for the iron complexes of 4-methyl-5-amino-1-formylisoquinoline thiosemicarbazone [29] and 2,2′-bipyridyl-6-carbothioamide [30].

Although iron depletion undoubtedly contributes to the toxicity of PIH analogs, it is unlikely to be the only mechanism. While the IC_{50} values of the analogs examined in this study varied over two orders of magnitude (Table 1), all chelators except PIH bound approximately the same amount of ^{59}Fe from labeled K562 cells (Fig. 6). In addition, the observation that ^{59}Fe binding by the chelators was similar at 10 and 100 μM (Fig. 5) indicates that maximal ^{59}Fe binding is achieved at very low chelator concentrations in K562 cells, at which some of the chelators cause no toxicity (Table 1). Thus, iron depletion alone cannot account for the observed relationship between toxicity and iron mobilization, and other mechanisms must be considered, as has been concluded previously [16].

PIH, SIH, and NIH have been demonstrated to induce apoptosis in Jurkat T lymphocytes and K562 cells [25], indicating that the effects of PIH analogs on cell growth (Table 1) are due to cytotoxic, as opposed to cytostatic, mechanisms. That incubation of K562 cells for 2 hr was sufficient to cause small losses in cell viability (Table 1) lends further support to this conclusion. It has been documented that other iron chelators, including desferrioxamine [15,31], induce apoptosis in cultured cells, suggesting that there may be common elements in their mechanisms of action.

The toxicity of the chelators toward K562 cells, assessed after 2- and 72-hr incubations (Table 1), demonstrated that the antiproliferative effects of the chelators increased as ^{59}Fe release from the cells decreased (Fig. 9A). PIH enters cells much more quickly than ^{59}Fe is mobilized [18]. Since the kinetics of iron binding by PIH analogs did not vary greatly (Fig. 3), it appears that membrane permeability of the chelators does not limit their access to intracellular compartments. Lipophilicity of the chelators, as measured by ethyl acetate/PBS partition coefficients, varied with both the aldehyde moiety (pyridoxal < salicylaldehyde < 2-hydroxy-1-naphthylaldehyde) and the substitution pattern of the hydrazide moiety (unsubstituted ≈ *ortho* < *meta* ≈ *para*). This property apparently determines the kinetics of release of iron–chelator complexes from K562 cells, most likely by modulating their affinities for the cell membrane [11], since the chelators that allow efficient release of ^{59}Fe from cells (see Figs. 3–6) have the lowest values of log *P* (Fig. 9B). Although an energy-dependent mechanism of release of the $FePIH_2$ complex has been proposed [18,32], evidence against such a mechanism has been reported for the iron complexes of analogs synthesized from salicylaldehyde and 2-hydroxy-1-naphthylaldehyde [32]. The Fe^{3+} complexes of these analogs, which may be expected to be much more lipophilic than $FePIH_2$ due to the high lipophilicity of the free chelators [19], are likely to leave the cell via passive diffusion [32]. A previous study demonstrated an inverse correlation between affinity for erythrocyte ghost membranes and the kinetics of release of the complexes from reticulocytes [11]. This finding suggests that, due to the fact that the more lipophilic iron–chelator complexes have higher affinities for membranes, their efflux from cells is blocked [11]. The accumulation of ^{59}Fe–chelator within the cell is correlated with toxicity (Fig. 9A), implicating the iron–chelator complexes in the mechanism of toxicity of the chelators.

The observation that BSA protects cells from the toxicity of PIH analogs (Fig. 8) supports the hypothesis that iron–chelator complexes are an active species. Since BSA remains in the extracellular medium, it can have no direct effect on intracellular Fe(chelator)$_2$ formation or efflux. The affinity of BSA for the iron complexes of PIH analogs is sufficient to prevent their binding to erythrocyte ghost membranes [11]. Thus, the most likely explanation of the effect of BSA on iron–chelator efflux is that it promotes the exit of the complexes from the membrane by serving as an extracellular sink, thereby reducing the intracellular concentration of the iron–chelator complex.

The concentration of intracellular ethanol-soluble ^{59}Fe, which presumably represents cytosolic ^{59}Fe–chelator, assessed after a 2-hr incubation with the chelators, is correlated with the antiproliferative effects of the chelators, assessed after a 72-hr incubation (Fig. 9A). Over long incubation times, the formation and efflux of Fe(chelator)$_2$

may reach an equilibrium with iron uptake from the culture medium, such that a steady-state level of intracellular iron–chelator is achieved. Thus, it may be expected that the steady-state level varies inversely with efflux, i.e. chelators that efflux iron slowly cause higher intracellular levels of iron–chelator, accounting for their increased toxicity (Table 1).

4.3. Summary

A detailed understanding of the mechanism of iron mobilization by PIH analogs, and its relationship to their toxicity, is important in the ongoing search for iron chelators with improved capacities to mobilize iron *in vivo*, without causing appreciable toxicity. In addition, chelators with strong antiproliferative effects may be of value as antitumor agents, as has been suggested previously [33]. The correlation of complex events such as chelator-mediated iron efflux and cell death to a simple property such as lipophilicity, which can be measured easily, may be valuable as an initial screen for the selection of analogs worthy of further investigation.

References

[1] Halliwell B, Gutteridge JM. Oxygen toxicity, oxygen radicals, transition metals and disease. Biochem J 1984;219:1–14.

[2] Richardson DR, Ponka P. The molecular mechanisms of the metabolism and transport of iron in normal and neoplastic cells. Biochim Biophys Acta 1997;1331:1–40.

[3] Olivieri NF, Brittenham GM. Iron–chelating therapy and the treatment of thalassemia. Blood 1997;89:739–61.

[4] Summers MR, Jacobs A, Tudway D, Perera P, Ricketts C. Studies in desferrioxamine and ferrioxamine metabolism in normal and iron-loaded subjects. Br J Haematol 1979;42:547–55.

[5] Ponka P, Borova J, Neuwirt J, Fuchs O, Necas E. A study of intracellular iron metabolism using pyridoxal isonicotinoyl hydrazone and other synthetic chelating agents. Biochim Biophys Acta 1979;586:278–97.

[6] Cikrt M, Ponka P, Necas E, Neuwirt J. Biliary iron excretion in rats following pyridoxal isonicotinoyl hydrazone. Br J Haematol 1980;45:275–83.

[7] Baker E, Richardson D, Gross S, Ponka P. Evaluation of the iron chelation potential of hydrazones of pyridoxal, salicylaldehyde and 2-hydroxy-1-naphthylaldehyde using the hepatocyte in culture. Hepatology 1992;15:492–501.

[8] Richardson DR, Tran EH, Ponka P. The potential of iron chelators of the pyridoxal isonicotinoyl hydrazone class as effective antiproliferative agents. Blood 1995;86:4295–306.

[9] Ponka P, Baker E, Edward JT. Effect of pyridoxal isonicotinoyl hydrazone and other hydrazones on iron release from macrophages, reticulocytes and hepatocytes. Biochim Biophys Acta 1988;967:122–9.

[10] Blaha K, Cikrt M, Nerudova J, Fornuskova H, Ponka P. Biliary iron excretion in rats following treatment with analogs of pyridoxal isonicotinoyl hydrazone. Blood 1998;91:4368–72.

[11] Buss JL, Arduini E, Ponka P. Mobilization of intracellular iron by analogs of pyridoxal isonicotinoyl hydrazone (PIH) is determined by the membrane permeability of the iron–chelator complexes. Biochem Pharmacol 2002;64:1689–701.

[12] van Reyk DM, Sarel S, Hunt NH. *In vitro* effects of three iron chelators on mitogen-activated lymphocytes: identification of differences in their mechanisms of action. Int J Immunopharmacol 1992;14:925–32.

[13] Darnell G, Richardson DR. The potential of iron chelators of the pyridoxal isonicotinoyl hydrazone class as effective antiproliferative agents III: the effect of the ligands on molecular targets involved in proliferation. Blood 1999;94:781–92.

[14] Becker E, Richardson DR. Development of novel aroylhydrazone ligands for iron chelation therapy: 2-pyridylcarboxaldehyde isonicotinoyl hydrazone analogs. J Lab Clin Med 1999;134:510–21.

[15] Richardson DR, Milnes K. The potential of iron chelators of the pyridoxal isonicotinoyl hydrazone class as effective antiproliferative agents II: the mechanism of action of ligands derived from salicylaldehyde benzoyl hydrazone and 2-hydroxy-1-naphthylaldehyde benzoyl hydrazone. Blood 1997;89:3025–38.

[16] Richardson DR, Ponka P. The iron metabolism of the human neuroblastoma cell: lack of relationship between the efficacy of iron chelation and the inhibition of DNA synthesis. J Lab Clin Med 1994;124:660–71.

[17] Edward JT, Gauthier M, Chubb FL, Ponka P. Synthesis of new acylhydrazones as iron-chelating compounds. J Chem Eng Data 1988;33:538–40.

[18] Huang AR, Ponka P. A study of the mechanism of action of pyridoxal isonicotinoyl hydrazone at the cellular level using reticulocytes loaded with non-heme ^{59}Fe. Biochim Biophys Acta 1983;757:306–15.

[19] Edward JT, Ponka P, Richardson DR. Partition coefficients of the iron(III) complexes of pyridoxal isonicotinoyl hydrazone and its analogs and the correlation to iron chelation efficacy. Biometals 1995;8:209–17.

[20] Vyoral D, Petrak J. Iron transport in K562 cells: a kinetic study using native gel electrophoresis and ^{59}Fe autoradiography. Biochim Biophys Acta 1998;1403:179–88.

[21] Vitolo ML, Webb J, Saltman P. Release of iron from ferritin by pyridoxal isonicotinoyl hydrazone and related compounds. J Inorg Biochem 1984;20:255–62.

[22] Ponka P, Schulman HM, Wilczynska A. Ferric pyridoxal isonicotinoyl hydrazone can provide iron for heme synthesis in reticulocytes. Biochim Biophys Acta 1982;718:151–6.

[23] Laskey J, Webb I, Schulman HM, Ponka P. Evidence that transferrin supports cell proliferation by supplying iron for DNA synthesis. Exp Cell Res 1988;176:87–95.

[24] Djeha A, Brock JH. Uptake and intracellular handling of iron from transferrin and iron chelates by mitogen stimulated mouse lymphocytes. Biochim Biophys Acta 1992;1133:147–52.

[25] Buss JL, Neuzil J, Gellert N, Weber C, Ponka P. Pyridoxal isonicotinoyl hydrazone analogs induce apoptosis in hematopoietic cells due to their iron-chelating properties. Biochem Pharmacol, in press.

[26] Schulman HM, Hermes-Lima M, Wang EM, Ponka P. *In vitro* antioxidant properties of the iron chelator pyridoxal isonicotinoyl hydrazone and some of its analogs. Redox Rep 1995;1:373–8.

[27] Santos NC, Castilho RF, Meinicke AR, Hermes-Lima M. The iron chelator pyridoxal isonicotinoyl hydrazone inhibits mitochondrial lipid peroxidation induced by Fe(II)-citrate. Eur J Pharmacol 2001;428:37–44.

[28] Green DA, Antholine WE, Wong SJ, Richardson DR, Chitambar CR. Inhibition of malignant cell growth by 311, a novel iron chelator of the pyridoxal isonicotinoyl hydrazone class: effect on the R2 subunit of ribonucleotide reductase. Clin Cancer Res 2001;7:3574–9.

[29] Preidecker PJ, Agrawal KC, Sartorelli AC, Moore EC. Effects of the ferrous chelate of 4-methyl-5-amino-1-formylisoquinoline thiosemicarbazone (MAIQ-1) on the kinetics of reduction of CDP by ribonucleotide reductase of the Novikoff tumor. Mol Pharmacol 1980;18:507–12.

[30] Nocentini G, Federici F, Franchetti P, Barzi A. 2,2′-Bipyridyl-6-carbothioamide and its ferrous complex: their *in vitro* antitumoral activity related to the inhibition of ribonucleotide reductase R2 subunit. Cancer Res 1993;53:19–26.

[31] Simonart T, Degraef C, Andrei G, Mosselmans R, Hermans P, Van Vooren JP, Noel JC, Boelaert JR, Snoeck R, Heenen M. Iron chelators inhibit the growth and induce the apoptosis of Kaposi's sarcoma cells and of their putative endothelial precursors. J Invest Dermatol 2000;115:893–900.

[32] Richardson DR. Mobilization of iron from neoplastic cells by some iron chelators is an energy-dependent process. Biochim Biophys Acta 1997;1320:45–57.

[33] Richardson DR. Potential of iron chelators as effective antiproliferative agents. Can J Physiol Pharmacol 1997;75:1164–80.